AD_____

Award Number: W81XWH-09-1-0240

TITLE: An RNAi-enhanced logic circuit for cancer specific detection and destruction.

PRINCIPAL INVESTIGATOR: Ron Weiss

CONTRACTING ORGANIZATION: Massachusetts Institute of Technology
Cambridge, MA 02139-4301

REPORT DATE: February 2013

TYPE OF REPORT: Final

PREPARED FOR: U.S. Army Medical Research and Materiel Command
Fort Detrick, Maryland 21702-5012

DISTRIBUTION STATEMENT: Approved for Public Release;
Distribution Unlimited

REPORT DOCUMENTATION PAGE

Form Approved
OMB No. 0704-0188

1. REPORT DATE	2. REPORT TYPE	3. DATES COVERED
February 2013	Final	1 July 2009 – 27 January 2013

4. TITLE AND SUBTITLE

An RNAi-enhanced logic circuit for cancer specific detection and destruction.

5a. CONTRACT NUMBER

5b. GRANT NUMBER
W81XWH-09-1-0240

5c. PROGRAM ELEMENT NUMBER

6. AUTHOR(S)

Ron Weiss, Liliana Wroblewska, Zhen Xie

E-Mail: rweiss@mit.edu

5d. PROJECT NUMBER

5e. TASK NUMBER

5f. WORK UNIT NUMBER

7. PERFORMING ORGANIZATION NAME(S) AND ADDRESS(ES)

Massachusetts Institute of Technology
Cambridge, MA 02139-4301

8. PERFORMING ORGANIZATION REPORT NUMBER

9. SPONSORING / MONITORING AGENCY NAME(S) AND ADDRESS(ES)
U.S. Army Medical Research and Materiel Command
Fort Detrick, Maryland 21702-5012

10. SPONSOR/MONITOR'S ACRONYM(S)

11. SPONSOR/MONITOR'S REPORT NUMBER(S)

12. DISTRIBUTION / AVAILABILITY STATEMENT
Approved for Public Release; Distribution Unlimited

13. SUPPLEMENTARY NOTES

14. ABSTRACT

Modern breast cancer therapies utilize non-specific approaches to kill or remove cancerous cells, inflicting significant collateral damage to healthy cells. In response to the need for highly targeted detection and destruction of cancerous cells, we propose to implement multi-input genetic circuits that act as cell state classifiers based on mRNA or microRNA expression profiling. The mRNA sensing project is focused on the MCF-7 breast adenocarcinoma cell line. MCF-7 cells overexpress Gata3, NPY1R and TFF1 mRNA relative to healthy cells. Based on our bioinformatics analysis, taking into account the three biomarkers allows for dramatically improved specificity in comparison to targeting single genes. We therefore design a three-input AND gate that triggers a response only when all three biomarkers are expressed above a defined threshold. In second approach we implement transcriptional/post-transcriptional regulatory circuit that senses expression levels of a customizable set of endogenous microRNAs and computes whether to trigger a response if the expression levels match a pre-determined profile of interest. We have created a circuit that computes a complex abstract logic (miR1 AND miR2+3 AND NOT miR4 AND NOTmiR5 AND NOT miR6) and selectively triggers output response in HeLa but not in other cells.

15. SUBJECT TERMS
RNA interference, classifier circuit, induced apoptosis, cancer cell detection and destruction

16. SECURITY CLASSIFICATION OF:			17. LIMITATION OF ABSTRACT	18. NUMBER OF PAGES	19a. NAME OF RESPONSIBLE PERSON
a. REPORT	b. ABSTRACT	c. THIS PAGE			USAMRMC
U	U	U	UU	17	19b. TELEPHONE NUMBER *(include area code)*

Table of Contents

INTRODUCTION

Motivation and objective

Modern breast cancer therapies utilize non-specific approaches to kill or remove cancerous cells, inflicting significant collateral damage to healthy cells. In response to the need for highly targeted detection and destruction of cancerous cells, we propose to implement multi-input genetic circuits that act as cell state classifiers based on mRNA or microRNA expression profiling.

The mRNA sensing project is focused on the MCF-7 breast adenocarcinoma cell line. MCF-7 cells overexpress Gata3, NPY1R and TFF1 mRNA relative to healthy cells. Based on our bioinformatics analysis, taking into account the three biomarkers allows for dramatically improved specificity in comparison to targeting single genes (Figure 1). We therefore design a three-input AND gate that triggers a response only when all three biomarkers are expressed above a defined threshold.

In a second approach we implement transcriptional/post-transcriptional regulatory circuit that senses expression levels of a customizable set of endogenous microRNAs and computes whether to trigger a response if the expression levels match a pre-determined profile of interest. We have created a circuit that computes a complex abstract logic (miR1 AND miR2+3 AND NOT miR4 AND NOTmiR5 AND NOT miR6) and selectively triggers output response in HeLa but not in other cells.

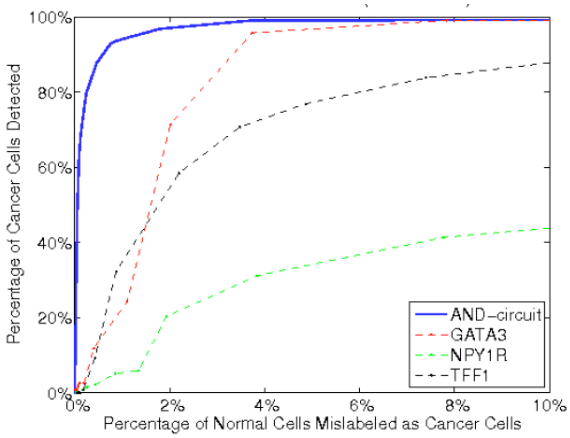

Figure 1: MCF7, breast adenocarcinoma cells overexpress Gata3, NPY1R and TFF1. Receiver operator characteristic (ROC) curves for single biomarkers and the AND-gate, visualize how taking into account three biomarkers improves specificity and selectivity.

BODY

I. Approach

I.a. mRNA-based cell classifier

In the first approach (Figure 2), the components of our proposed circuit include an apoptotic gene with an engineered regulatory sequence (RS), short interfering RNA (siRNA) or microRNA directed against the RS, and a set of additional short mRNA sequences, mStaples. Each mStaple molecule is complementary to a specific cancer biomarker and partially complementary to a portion of the RS. The role of mStaple is to regulate siRNA mediated degradation of the apoptotic gene. In the absence of mStaple, the RS forms a stem loop where the siRNA binding site is hidden and does not allow for siRNA binding and degradation of the mRNA. As a result, the cell undergoes apoptosis. When the mStaple binds to the RS, it enforces a conformational change of the sequence and exposes siRNA binding site.

The mRNA of the apoptotic gene is degraded and the cell survives. The expected behavior is therefore abundance of the mStaple in normal cells and it's shortage in cancer cells. In our system the mStaple is expressed similarly in all cell types, but it's availability for binding of the RS depends on the level of endogenous genes – cancer biomarkers. The mStaple binds preferentially to the biomarker mRNA and with lower affinity to the RS. In normal cells with low biomarker levels some of the mStaple will be bound by the biomarker and some will target the RS to expose the siRNA binding sequence (Figure 2B). In cancer cells, when the biomarker level is high, the mStaple will be titrated away, causing no disruption in expression of the apoptotic gene, and ultimately cell death (Figure 2A). For testing purposes, we replace the killer gene with a reporter, EYFP gene in the first implementation of the circuit.

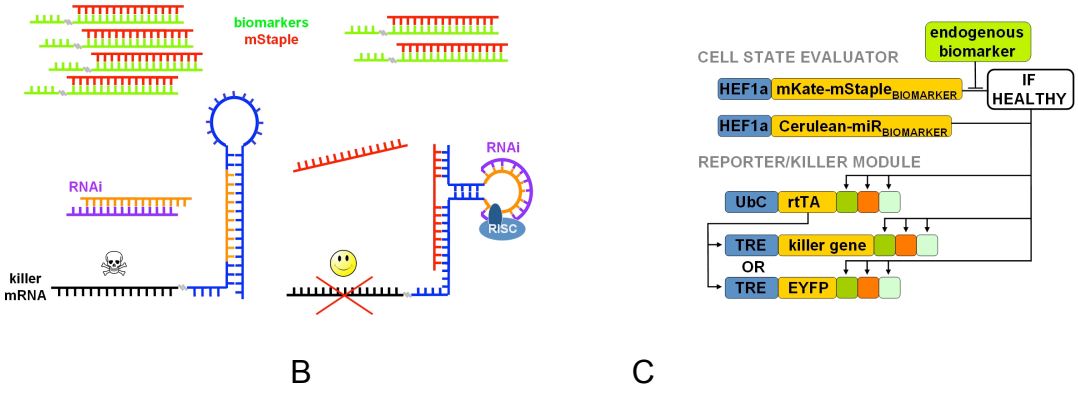

A B C

Figure 2: RNAi-based logic circuit, approach I. Expression of the apoptotic (killer) protein is dependent on the endogenous biomarker mRNA. Circuit logic in cancer cells (A) and normal cells (B); circuit implementation (C)

I.b. microRNA-based cell classifier

In our second approach we took advantage of the increasing knowledge of microRNA profiles for different cell types, including various diseased cell states. We have constructed multi-input cell classifier circuit [1], Figure 3, that ascertains whether the expression profile of six endogenous microRNAs matches a predetermined reference profile characteristic of the HeLa cervical cancer cell line. A match identifies the cell as HeLa and triggers apoptosis. The model system can be later customized to recognize and target any cell state of interest, including different types of cancer.

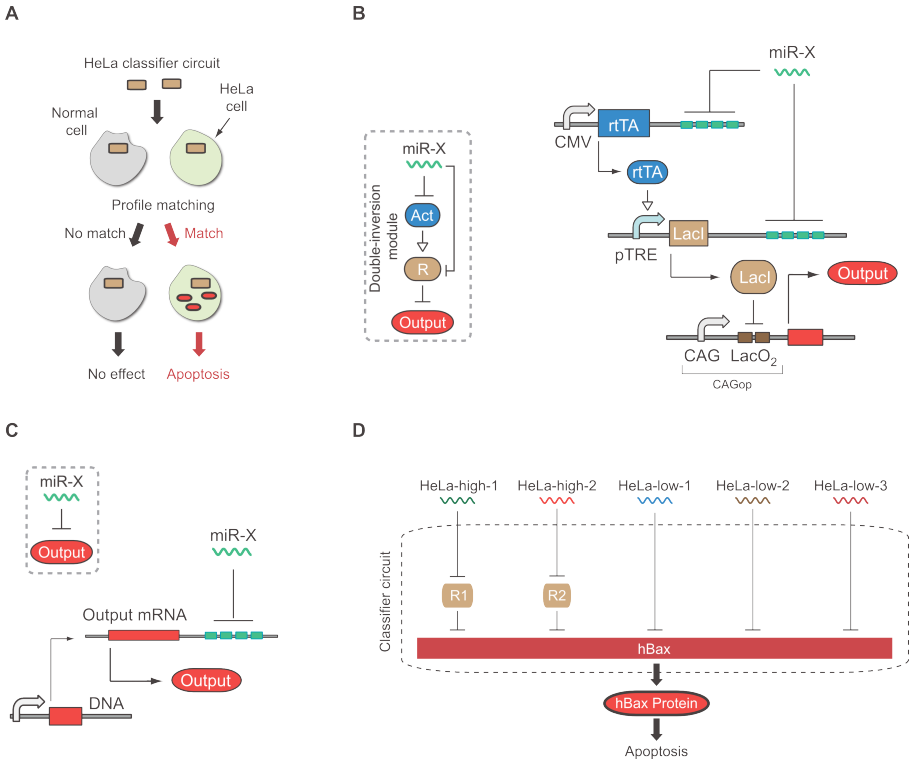

Figure 3: Schematic representation of a HeLa-specific classifier circuit operation (A). High-level and detailed description of 'double-inversion' module for sensing HeLa-high microRNAs. Act, activator; R, repressor (B). High-level and detailed description of HeLa-low microRNA sensor (C). Integrated multi-input classifier. R1, R2 - double-inversion modules (D). The entire network implements a multi-input AND-like logic function for identification and selective killing of HeLa cells through regulated expression of hBax.

II. Results

II.a. mRNA-based cell classifier: Circuit design and modeling

We have carefully designed the regulatory sequence (RS) at the 3'UTR of the killer/reporter gene to program a conformational change of the RS in the presence of mStaple molecules. DNA and RNA structures are much easier to predict and design than protein structures and the folding rules are well established in the DNA origami field. The mStaple molecule binds to the Gata3 gene with perfect complementarity and it is only partially complementary to the designed regulatory sequence. Therefore, it will bind to the killer/reporter gene 3'UTR with lower affinity, and preferentially only after all Gata3 binding sites have been satisfied. Upon mStaple binding, the RS mRNA fragment undergoes a conformational change, exposing siRNA binding site. Such design allows for Dicer mediated degradation of the killer/reporter mRNA in cells with low biomarker levels. In Figure 4 we show predicted structures of a single biomarker, Gata3-dependent regulatory sequence alone (A) and in the presence of mStaple (B).

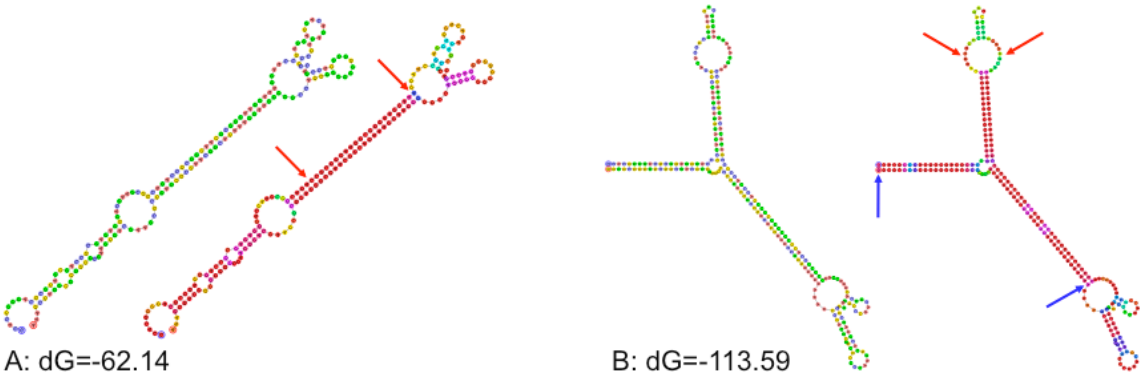

Figure 4: Secondary structure prediction for Gata3-dependent regulatory sequence with mfold [2,3]. Left panels are color coded according to nucleotide composition, and right panels according to structure formation probability (red indicates high). In the absence of mStaple (A), siRNA target site (within red arrows) is hidden by perfect base-pair complementarity. To simulate the presence of mStaple, its sequence has been added to the regulatory element sequence with a (polyA)x6 linker (B). Upon mStaple binding (blue arrows), a more stable structure is formed and the siRNA target site gets exposed.

II.b. mRNA-based cell classifier: mStaple expression

We designed a disruptive artificial intron in the coding sequence of the far-red fluorescent protein mKate to express the Gata3 mStaple. Intron-feature sequences – donor site, branch point, poly-pyrimidine tract, and acceptor site – were selected based on previously reported works. The donor site begins the 5' exon-intron junction, and the acceptor site ends the 3' intron-exon junction. Among the donor and acceptor sequences found in literature our intron features were chosen according SplicePort [4], an online analyzer that detects the likelihood of splicing to occur at a specific donor and acceptor site given the sequence context. The final Gata3 mStaple intron design was 5'-GTAAGTGGTCCAAAGGACAGGCTGGATGGCGGGTGCATCGGCGTGGGCGTGGTACTAACTTAA CTCGAGTCTTCTTTTTTTTTTTTCACAG-3', the features of which were donor site, Gata3 mStaple, branch point, an in-frame stop codon, XhoI cut site, poly-pyrimidine tract, and acceptor site, respectively. The 96bp Gata3 mStaple intron sequence was inserted into mKate between positions 271 and 272 via PCR.

The fluorescent protein, mKate, can only be produced when splicing does occur. In Figure 5 we show FACS results for cells infected with Hef1a-mKate, Hef1a-mKate-Gata3intron, and Hef1a-mKate-Gata3intron-21 constructs. The last construct is similar to Hef1a-mKate-Gata3intron, but includes additional 21bp sequence between the branch point and the acceptor site. Gata 3 mStaple intron is relatively short compared to typical intronic sequences, and we wanted to test if the intron size increase has any effect on the splicing efficiency.

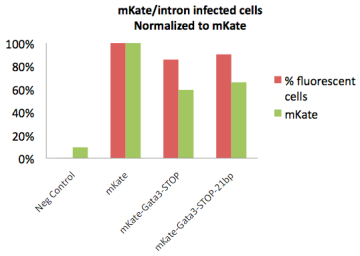

Figure 5: FACS results for 293FT cells infected with constructs expressing mKate (Hef1a-mKate) or Gata3 mStaple as an intron within mKate sequence (Hef1a-mKate-Gata3intron, Hef1a-mKate-Gata3intron-21 constructs). Fluorescence levels for the intronic constructs suggest 60-70% splicing efficiency.

Based on the FACS data, the splicing efficiency is about 60-70%. To finally confirm that no fluorescence can be produced from the non-spliced intronic mKate mRNA, we also created two additional constructs: Hef1a-half-mKate containing only the first exon of the protein and Hef1a-

mKate-STOP, that has a STOP codon in place of the intronic sequence. As expected, transfection of 293FT cells with these constructs produced no fluorescence. The cells expressing Gata3 mStaple display normal morphology and viability.

II.c. mRNA-based cell classifier: Non-integrating lentivirus

We proposed a non-integrating lentivirus as a potential delivery vehicle for the circuit-based therapeutics. To eliminate insertional mutagenesis but still allow circularization of the viral genome for packaging, reverse transcription after infection, and nuclear import of the preintegration complex, we used a type I lentiviral mutant integrase. Non-integrating lentivirus is a promising candidate for efficient gene delivery due to its retention of desirable virus activities like packaging and reverse transcription without the risk of non-specific integration into the host DNA [5]. Integration of the viral DNA is mediated by the 32kd viral integrase (IN) which is encoded by the pol gene [5]. Integrase catalyzes the reaction of 3'-OH groups at the viral DNA ends attacking the phosphodiester bonds on the host DNA by several mechanisms [6]. The D64-D116-E152 catalytic triad in the IN core domain is highly conserved and essential for integration. Residue Q148 is involved in binding to the viral DNA at the U3 and U5 sites of long terminal repeats, whereas N120 and W235 are responsible for binding to the host DNA [5]. Acetylation of three lysines in the C terminus, K264, 266, and 273, enhance viral strand transfer activity by increasing the binding affinity to the host DNA [7]. A number of past studies have shown that point mutations of these crucial residues have led to various degrees of integrase deficiency. For our proposal, we introduced a combination of these point mutations to generate class I mutants that are deficient in integration but not in assembly or reverse transcription [6]. A mutant of IN was created and sequenced: D64V + N120L + W235E.
To evaluate the expression of eGFP over time, HEK-293FT cells were infected with UbC-EGFP packaged with the IN mutant as well as wild-type IN. Flow cytometry was used to measure EGFP expression for 11 days after infection with n = 3 for each vector. Cells infected with the D64V + N120L + W235E mutant IN vector showed an 18-fold reduction in EGFP expression compared to wild-type at 11 days after transduction, comparable to background levels (Figure 6). Transduction of EGFP expression by wild-type integrase actually increased over the course of the experiment, indicating successful integration in these dividing cells. We engineered the mutant integrase to deliver the circuit transiently to all cells. Successful circuit operation in the particular cancer cell line that we target would activate the apoptotic pathway even with a mutant integrase whereas other cell types would not be affected by circuit operation; ultimately this circuit would be degraded and diluted with no permanent effects.

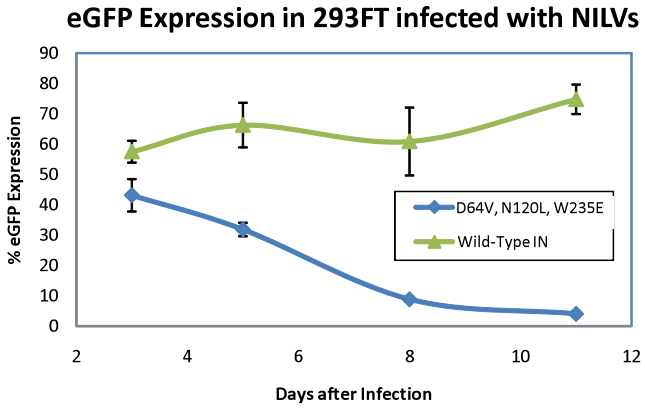

Figure 6: Experimental data for non-integrating lentivirus demonstrating how GFP expression from a constitutive promoter is initially high using both a wild type integrase and a mutant, while over the course of 10 days GFP intensity is reduced to essentially auto-fluorescence levels for the NI-lentivirus.

II.d. mRNA-based cell classifier: Regulatory sequence in the 3'UTR hides miRNA binding site and inhibits gene knockdown

We have created and tested all the components of the sensing circuit, using artificial, orthogonal to mammalian expression system and very efficient microRNA targeted against firefly luciferase, miRFF4 [8], and mStaple complementary to Gata3 gene, that is one of the best breast cancer biomarkers.
First, to verify that the designed regulatory sequence is capable of hiding and exposing the microRNA binding site we have tested EYFP-3'UTR knockdown, where the 3'UTR contained one of the following:
(a) 4xFF4, 4 repeats of FF4 target sequence (maximal knockdown),
(b) SSL-FF4, short stem loop (SSL) containing FF4 target site – fragment of RS simulating mStaple bound conformation (knockdown expected),
(c) LSL-FF4, long stem loop (LSL) containing FF4 target site – the full regulatory sequence (knockdown not expected without mStaple present).

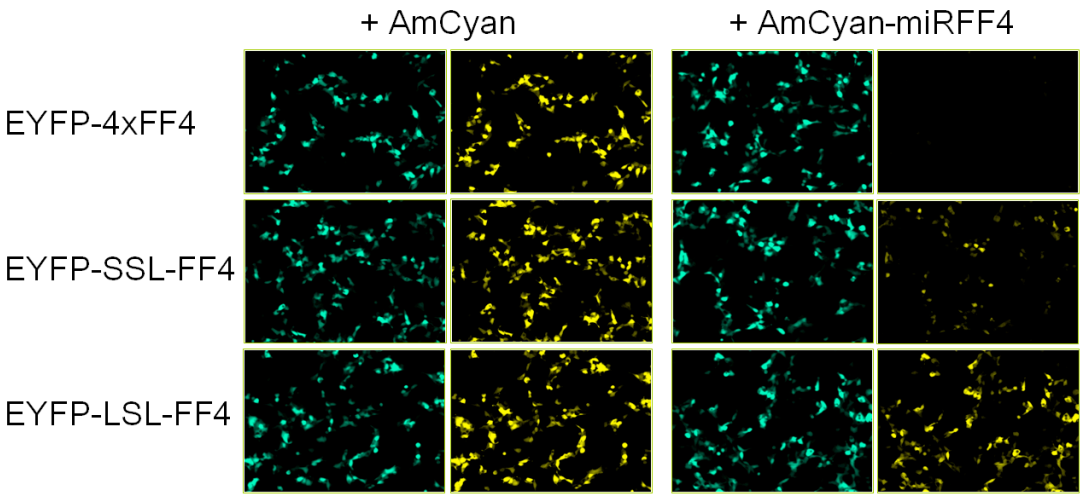

Figure 7: 293FT cells were co-transfected with TRE-EYFP-3'UTR and AmCyan or AmCyan-miRFF4 expressing constructs. As designed, the conformation LSL prevents gene knockdown.

The results agree with our predictions very well. The full regulatory sequence hides siRNA target site, whereas the shorter sequence that can only form SSL and therefore simulates the presence of mStaple, exposes the target site (Figure 7).

II.e. mRNA-based cell classifier: mStaple dependent gene knockdown

In the next step we tested the system with the Gata3 mStaple. We previously showed that the mStaple causes a conformational change of our designed regulatory sequence in vitro. Now we also show that the designed regulatory sequence is capable of the mStaple-regulated conformational change that results in siRNA mediated reporter mRNA degradation in vivo (Figure 8). When a reporter gene with the regulatory sequence in the 3'UTR is co-transfected with either just the targeting siRNA-FF4, or the Gata3 mStaple and a nonsense siRNA, the gene knockdown is lower than in the case of simultaneous co-transfection of siRNA-FF4 and the Gata3 mStaple.

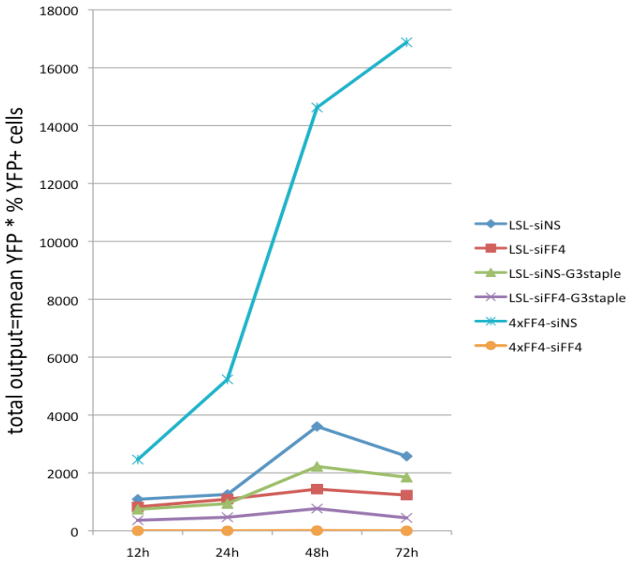

Figure 8: Best results for the mRNA sensing sub-circuit; YFP is the actuation gene, LSL (long stem loop) is our designed 3'UTR regulatory sequence, siNS-nonsense siRNA, siFF4-FF4 siRNA, 4xFF4 are 4 repeats of the siFF4 target sequence attached in the 3'UTR instead of LSL (control).

II.f. hBax induced apoptosis

In the final design of our circuit, a reporter gene will be replaced with a pro-apoptotic protein. For that purpose we have explored a few possibilities including diphtheria toxin, a monomeric protein secreted by *Corynebacterium diphtheriae*, and pro-apoptotic members of Bcl-2 family: mBax (Mus musculus), hBax (Homo sapiens), and its mutant hBax-S184A [9]. A plasmid containing the tested gene was transfected into HEK 293FT cells and cell death was monitored by comparison with cells transfected with an equal amount of a plasmid expressing EGFP. The pro-apoptotic gene-containing construct was either cotransfected with an EGFP expressing plasmid (diphtheria toxin and mBax) or in the case of hBax, expressed as an hBax-EGFP fusion. The diphtheria toxin appeared to be too potent and its expression is not tolerated with any promoter leakiness. The mBax, on the other hand, did not exhibit sufficient potency and only after 4 days of expression some cell toxicity was observed. The hBax and its mutant seem to be the best choices, as they induce apoptosis quickly and strongly, and potency can be regulated by mutagenesis [9] or compensated by co-expression of cell survival promoting proteins such as Bcl-2 or Bcl-X_L. The results showing hBax induced apoptosis are presented in Figure 9.

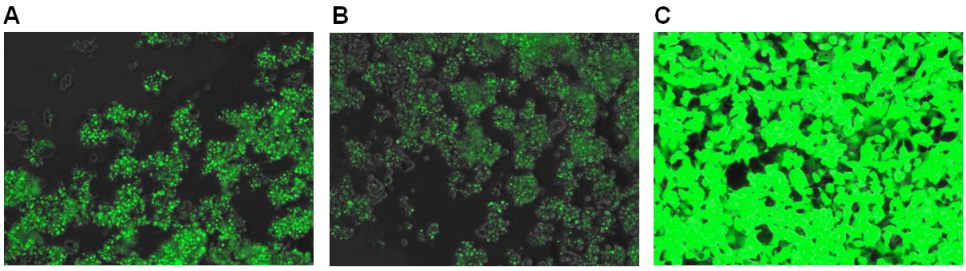

Figure 9: hBax induced apoptosis: 293FT HEK cells were imaged 48h post transfection with constructs constitutively expressing (A) EGFP-hBax fusion protein, (B) EGFP-hBax-S184A fusion, (C) and EGFP alone.

II.g. microRNA-based cell classifier: 6-microRNA profile can differentiate HeLa cells from other cell types

To choose HeLa markers for the reference profile and analyze expected circuit performance, we created a mathematical model consisting of a multi-variable circuit response function that uses experimentally derived responses of individual sensors to their miRNA inputs [1]. We first evaluated HeLa-high marker combinations from the set of the top 12 candidates determined by analyzing expression data from the MicroRNA Atlas [10], (Figure10A). On the basis of reasonable assumptions regarding sensor response parameters, we found that using miR-21 together with a composite marker that includes both miR-17 and miR-30a (miR-17-30a) results in at least a fivefold difference between circuit output in HeLa cells and the output in all but a few healthy cell types profiled in the MicroRNA Atlas [1,10]. We then searched for HeLa-low markers and found that miR-141, miR-142(3p), and miR-146a are highly expressed in the potentially misclassified cell types but unexpressed in HeLa (Figure 10B). We also computed selectivity of all possible marker subsets and found that it steadily increases as the number of markers goes from one to five (Figure 10C). With all inputs included, the response function is well approximated by a Boolean expression:

miR-21 AND miR-17-30a AND NOT(miR-141) AND NOT[miR-142(3p)] AND NOT(miR-146a)

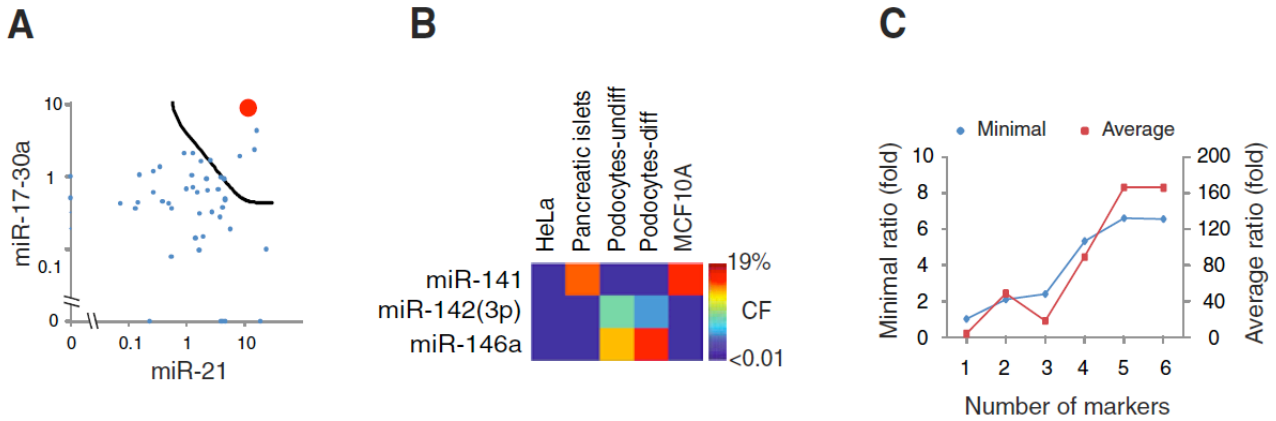

Figure 10: HeLa-specific microRNA profile. (A) Simulated output levels of a two-input circuit with miR-21 and miR-17-30a inputs. Each dot represents a particular cell type, and the contour line shows input combinations that result in 20% output relative to HeLa cells (red dot). Dots above the contour line represent "false-positive" cell types for this specific circuit configuration. The numbers on the axes are given in cloning frequency (CF) units. (B) CF of selected HeLa-low markers in false-positive cell types. (C) Circuit selectivity as a function of the number of markers. For a given number of markers (x axis), we computationally generate all possible classifier circuits by choosing subsets of markers from the set of six chosen markers and evaluate circuit output in HeLa cells and in the profiled healthy cell types. We then choose a circuit that maximizes the worst output ratio between HeLa and all non-HeLa cell types ("minimal") and also calculate the average output ratio for this circuit ("average").

II.h. microRNA-based cell classifier: The classifier circuit activates output production in HeLa cells only

We designed a sensor motif for HeLa-high markers comprising a "double-inversion" module that allows output expression only if the marker is present at or above its level in HeLa cells but efficiently represses the output if the marker's level is low (Figure 1 and11). The design is based on our previously described module that consists of the small interfering RNA (siRNA)–targeted transcriptional Lac repressor (LacI) and a LacI-controlled promoter CAGop (CAG promoter followed by an intron with two LacO sites) [11]. We improved the ON:OFF ratio of our original design to approximately 8- to 10-fold by introducing a reverse tetracycline controlled transactivator (rtTA) to

control LacI and by targeting both the repressor and the activator using miRNA in a feed-forward loop (Figure 11). A HeLa-low marker sensor was implemented by fusing four repeats of fully complementary target sites into the output's 3′-untranslated region (3′-UTR). A complete classifier circuit consists of a set of HeLa-high and HeLa-low marker sensors all arranged to target the same output (Figure 11).

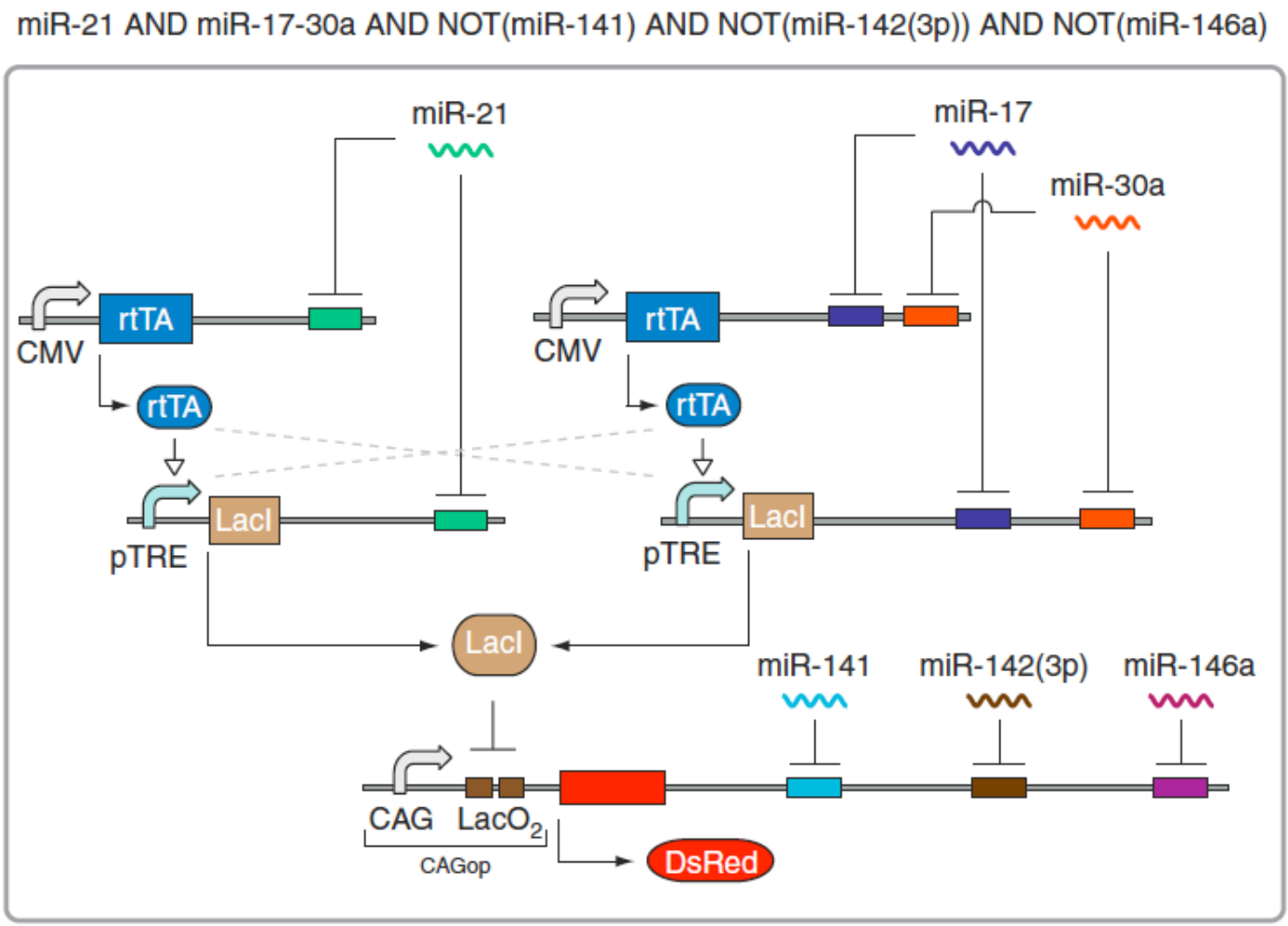

Figure 11: Schematics of the complete HeLa classifier circuit. For simplicity, four adjacent miRNA target sites are shown as a wider box, and DNA/RNA species are lumped together. Two double-inversion modules for HeLa-high markers and three sensors for HeLa-low markers are shown. rtTA crosstalk is indicated with dotted lines. The logic "computed" by the circuit is shown on top.

To test the circuit we performed fluorescence reporter assays in 7 different cell lines. The complete circuit performs as desired experimentally, resulting in an output that is substantially higher in HeLa cells both in absolute and relative units as compared with the other cell lines in the set (Figure 12). Analysis reveals that for the cell types assayed, the circuit operates well because of one of two conditions: At least one sensor exhibits a response in a non-HeLa cell that is an inverse of that sensor's response in a HeLa cell [human embryonic kidney (HEK) 293, MCF-7, and SH-SY5Y], or a sufficient number of responses deviate moderately from the ones observed in HeLa cells (DAOY, SKBR3, and T47D). The classifier's output in T47D is much better than the prediction suggesting that further model refinement may be necessary.

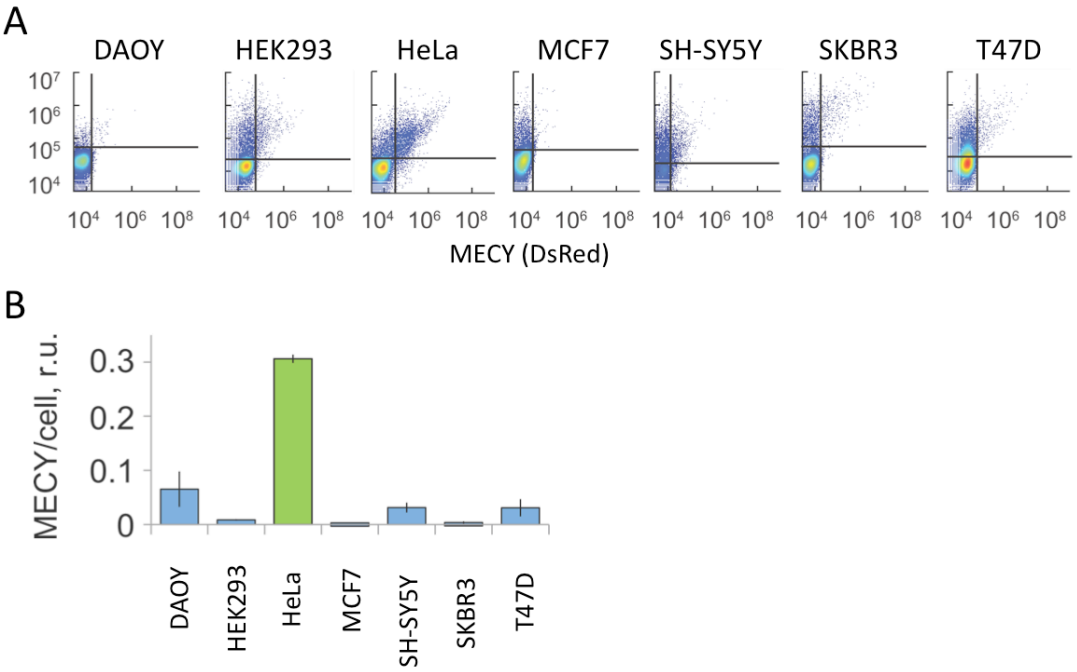

Figure 12: The classifier circuit identifies HeLa cells in a fluorescence reporter assay; representative flow cytometry scatter plots (A), relative output levels (B). Bars show mean ± SD from at least three independent replicates.

II.i. MicroRNA-based cell classifier: in mixed cell culture our circuit identifies and specifically kills HeLa cells

Lastly, we tested whether the circuit can selectively trigger apoptosis by regulating expression of human Bcl-2–associated X protein hBax. We replaced the circuit fluorescent output with the apoptotic protein hBax, and tested it's performance in a mixed population of HEK 293 and HeLa cells. When circuit expressing hBax output was transfected into a mixed cell culture, only HeLa cells were selectively killed according to our assay (Figure 13).

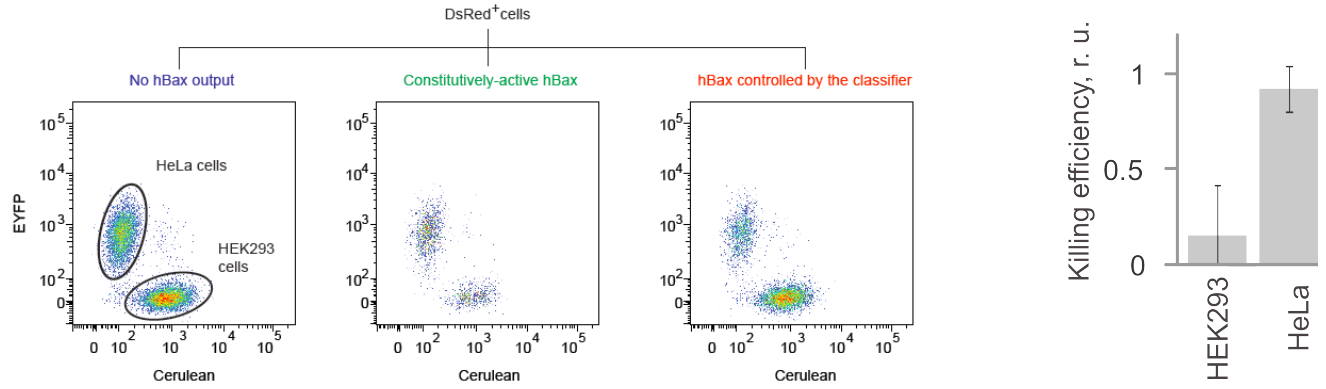

A B

Figure 13: Apoptosis assay in HeLa and HEK293 cell lines; Mixed culture of Hela cells stably expressing yellow fluorescent protein (FP) and HEK293 cells stably expressing cerulean FP were co-transfected with circuit parts. The resulting fluorescence distribution was compared to a control mixed culture to assess killing efficiency (A). Normalized killing efficiency (B).

II.j. microRNA-based cell classifier: Moving towards therapy, single plasmid version of the classifier

Our microRNA cell profiler presents one of the most sophisticated in-vivo biosensors reported to date. Although, many challenges still need to be overcome before this or other synthetic biology circuits can be used in the clinic. Moving the work forward, we chose to focus on improving the implementation of the classifier to make it simpler for delivery and more suitable for future possible applications (therapy). Additionally we studied microRNA profiles of other diseased cell states with the aim of creating multiple therapy-relevant classifier circuits.

In the first implementation, the profiler circuit was delivered in co-transfection of 5 plasmids and the 6-th plasmid was used as a transfection control (Figure 14, blue shade). This configuration is far from optimal for possible applications, given that all the parts need to be present in order for the classifier to be fully functional. In the first approach we created and tested a single-plasmid version of the classifier circuit using an assembly method, newly developed in our lab (12). In short, promoters, genes and the appropriate 3'UTR regulatory sequences are recombined using standard Gateway cloning (13) and inserted in a specially designed destination vector to create one transcription unit (TU) position vectors. In the second step the position vectors are assembled together with a carrier vector (new backbone) in a single Gibson assembly reaction (14). During the assembly process the backbones of position vectors are disregarded, and the final vector contains TU1-TU2-…-TUx. Additionally, each position vector contributes a chromatin insulator upstream of the TU (cSH4), to prevent interference between the parts.

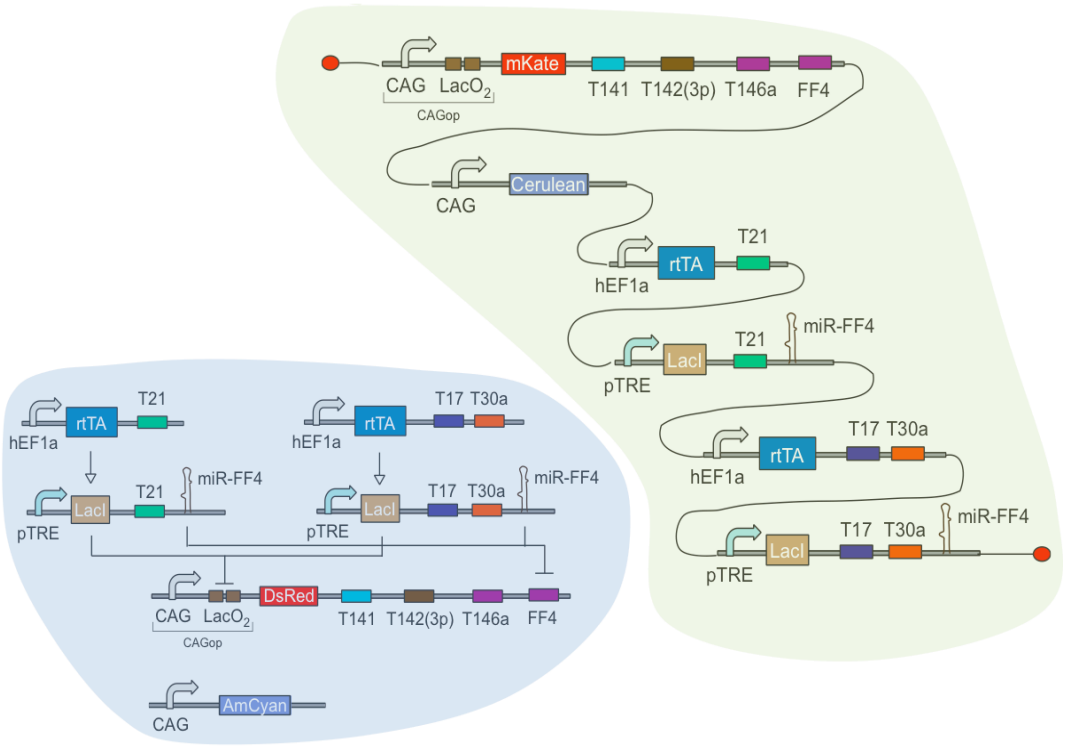

Figure 14: microRNA-based HeLa classifier circuit in a multi-plasmid (gray shade) and single plasmid (green shade) configuration.

We have tested performance of the single-plasmid version of our microRNA classifier circuit by transient transfection in HEK 293 and HeLa cells. When compared with the multi-plasmid co-transfection data (Figure 15) the results are very encouraging. Single-plasmid classifier performs at least as good as the original circuit version with a slightly lower false positive rate (lower HEK293/HeLa overlap for the circuit controlled output).

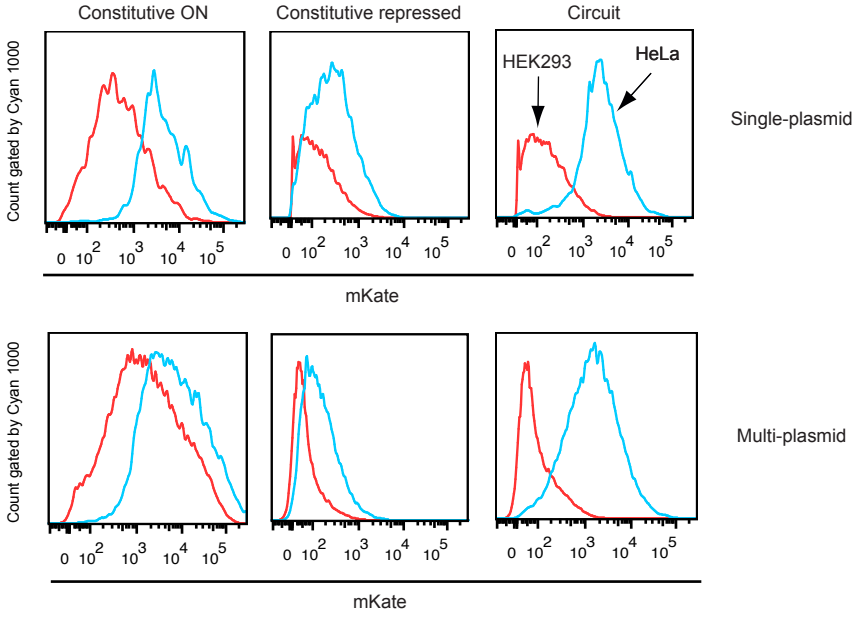

Figure 15: Performance of the microRNA classifier in single-plasmid configuration, as compared with multi-plasmid co-transfection: representative FACS histograms.

III. Outreach

The following students were involved in the project and mentored:
Genia Dubrovsky (junior project, 2009)
Anna Igorevna Podgornaia (rotation student, 2009)
Hattie Chung (Amgen scholar, 2010)

KEY RESEARCH ACCOMPLISHMENTS

mRNA-based classifier circuit:

- Design and experimental verification of the 3'UTR regulatory sequences SSL and LSL that can expose or hide microRNA target site regulating gene knockdown;
- Demonstration of gene knockdown regulation by a short RNA oligunucleotide, mStaple.

microRNA-based classifier circuit:

- Design and experimental verification of a sophisticated multi-input microRNA-based cell classifier circuit that can specifically activate output production in HeLa;
- Demonstration of specific killing of HeLa cells when a mixed culture is transfected with the classifier circuit that controls production of a pro-apoptotic gene hBax.
- Development and testing of a single-plasmid version of the microRNA classifier circuit as a step forward in the direction towards its therapeutical application.

REPORTABLE OUTCOMES

- Within the scope of the research we have created the following stable cell lines:
  HEK 293FT:TRE-EYFP-4xFF4 (microRNA-dependent TetON system)

HEK 293FT:TRE-EYFP-4xT1 (microRNA-dependent TetON system)

HEK 293FT:UbC-rtTA3-4xFF4 (microRNA-dependent TetON system)

HEK 293FT:TRE-EYFP-4xFF4:UbC-rtTA3-4xFF4 (microRNA-dependent TetON system)

HEK 293FT:TRE-EYFP (TetON system)

HEK 293FT:UbC-rtTA3-2A-Hygromycin (TetON system)

HEK 293FT:TRE-EYFP-4xFF4:UbC-rtTA3-2A-Hygro (microRNA-dependent TetON system)

HEK 293FT:Hef1a-AmCyan-miRFF4 (microRNA expression)

HEK 293FT:Hef1a-AmCyan

HEK 293FT:CMV-Bcl2-UbC-Phleomycin (Bax/Bcl apoptotic system)

HEK 293FT:Hef1a-mKate-Gata3intron (splicing dependent mStaple expression)

Glossary of terms:

CMV, Hef1a, UbC – constitutive promoters

TRE – tetracycline response element, inducible promoter

rtTA3 – transcription factor, TetON system

EYFP, AmCyan, mKate – yellow, cyan and red fluorescent proteins

Hygromycin, Phleomycin – antibiotic resistance markers

- The work has been presented on the following conferences:

- The American Society for Cell Biology annual meeting, Philadelphia, PA, Dec 11-15, 2010
- SB5.0: The Fifth International Meeting on Synthetic Biology, Stanford, CA, Jun 14-17, 2011
- Era of Hope, Orlando, FL, Aug 2-5, 2011

- The microRNA classifier work have been published:

  Xie, Z., Wroblewska, L., Prochazka, L., Weiss, R., and Benenson, Y. (2011). Multi-input RNAi-based logic circuit for identification of specific cancer cells. *Science* 333, 1307-1311.

- Patents filed:

  (1) U.S. S/N: 12/587,994 “Detection And Destruction Of Cancer Cells Using Programmed Genetic Vectors” M&C Ref. No.: WEISS-16603/MIT-16791

  (2) NP 002806-067600-P: "Multiple Input Biologic Classifier Circuits for Cells"

CONCLUSION

We have predicted and demonstrated experimentally that microRNA dependent gene knockdown can be regulated by 3’UTR secondary structure of the target gene. The secondary structure can be changed with the help of exogenously added short RNA oligonucleotide, mStaple. Based on that, we created an mRNA sensing circuit that shows promising results in a fluorescent assay, although still requires further optimization.

We have also designed and successfully implemented microRNA-based classifier circuit for selective

detection and destruction of cancer cells. Our classifier identifies and kills HeLa cells among other cell lines by compiling information about levels of specific microRNAs in the cell and triggering production of the output (fluorescent or pro-apoptotic protein) only when a certain microRNA profile is matched. Building on new circuit assembly technologies, we have created a single plasmid version of the classifier circuit. The new circuit configuration did not influence its performance and made it more manageable for future possible applications (therapy).

REFERENCES

1. Xie, Z., Wroblewska, L., Prochazka, L., Weiss, R., and Benenson, Y. Multi-input RNAi-based logic circuit for identification of specific cancer cells. *Science* 333, 1307-1311, (2011)
2. M. Zuker, Mfold web server for nucleic acid folding and hybridization prediction. *Nucleic Acids Res.* 31 (13), 3406-15, (2003)
3. D.H. Mathews, J. Sabina, M. Zuker & D.H. Turner, Expanded Sequence Dependence of Thermodynamic Parameters Improves Prediction of RNA Secondary Structure. *J. Mol. Biol.* 288, 911-940 (1999)
4. R. Islamaj Dogan, L. Getoor, W.J. Wilbur and S.M. Mount SplicePort: An Interactive Splice-Site Analysis Tool, *Nucleic Acids Research*, 35, 1-7, (2007)
5. L. Apolonia, S.N. Waddington, C. Fernandes, N.J. Ward, G. Bouma, M.P. Blundell, A.J. Thrasher, M.K. Collins, N.J. Philpott, Stable Gene Transfer to Muscle Using Non-integrating Lentiviral Vectors. *Molecular Therapy,* 15(11):1947-1954, (2007)
6. N.J. Philpott, A.J. Thrasher, Use of Nonintegrating Lentiviral Vectors for Gene Therapy, *Human Gene Therapy,* 18:483-489, (2007)
7. A. Cereseto, L. Manganaro, M.I. Gutierrez, M. Terreni, A. Fittipaldi, M. Lusic, A. Marcello, M. Giacca, Acetylation of HIV-1 integrase by p300 regulates viral integration, *The EMBO Journal*, 24:3070-3081, (2005)
8. M. Leisner, L. Bleris, J. Lohmueller, Z. Xie & Y. Benenson, Rationally designed logic integration of regulatory signals in mammalian cells, *Nat Nanotech* 5, 666-670, (2010)
9. A. Nechushtan, C.L. Smith, Y.T. Hsu, R. J. Youle, Conformation of the Bax C-terminus regulates subcellular location and cell death. *EMBO J*. 18(9):2330-41, (1999)
10. P. Landgraf et al., A mammalian microRNA expression atlas based on small RNA library sequencing, *Cell* 129(7): 1401, (2007)
11. K. Rinaudo et al., A universal RNAi-based logic evaluator that operates in mammalian cells, *Nat. Biotechnol.* 25(7): 795, (2007)
12. Guye P*, Li Y*, Wroblewska L, Duportet X, Weiss R (* equal contribution), Rapid, modular, and reliable construction of complex mammalian gene circuits" (2013, submitted).
13. Sasaki, Y et al., Evidence for high specificity and efficiency of multiple recombination signals in mixed DNA cloning by the Multisite Gateway system, *J Biotech* 107.3, 233-243, (2004)
14. Gibson, DG et al., Enzymatic assembly of DNA molecules up to several hundred kilobases, *Nat Meth* 6.5, 343-345, (2009)

APPENDICES

Xie, Z., Wroblewska, L., Prochazka, L., Weiss, R., and Benenson, Y. (2011). Multi-input RNAi-based logic circuit for identification of specific cancer cells. *Science* 333, 1307-1311